American Journal of Biomedical Sciences
ISSN: 1937-9080
nwpii.com/ajbms

Three Dimensional Ordered Macroporous Electrochemical Sensor for Dopamine Recognition and Detection

Xianwen Kan*, Chen Li, Hong Zhou, Anhong Zhu, Zonglan Xing, Zhe Zhao and Guilin Xu

College of Chemistry and Materials Science, Anhui Key Laboratory of Chemo-Biosensing, Anhui Normal University, Wuhu, P.R. China
***Corresponding Author:**
Xianwen Kan
Professor of College of Chemistry and Materials Science
Anhui Normal University
Wuhu, Anhui, 241000
P. R. China
Tel: +86 553 3883513
Fax: +86 553 3869303
E-mail: kanxw@mail.ahnu.edu.cn

Received: 17 February 2012; | Revised: 22 March 2012; | Accepted: 16 April 2012

Abstract

A novel kind of electrochemical sensor was developed by combining the molecularly imprinting and silica colloidal crystal template (SCCT) techniques in this work. Pyrrole was electropolymerized onto the SCCT modified glassy carbon electrode (GCE) surface in the presence of dopamine (DA). Then a three dimensional ordered macroporous (3DOM) structured molecularly imprinted polymer (MIPs) electrochemical sensor (3DOM-MIPs/GCE) was obtained by etching of silica microspheres and extracting of DA successively. Scanning electron microscope (SEM) and electrochemical impedance spectroscopy (EIS) were employed to characterize the prepared process of the sensor. Due to the high surface area and thin wall of 3DOM imprinted polymers on the electrode surface, the prepared sensor provided much more efficient imprinted sites and exhibited a fast binding dynamics, good specific adsorption capacity, and high selective recognition to template molecule. And the sensor could also be used for DA determining. Peak current of DA varied linearly with the concentration of DA in the range of 2.0×10^{-6} ~ 2.3×10^{-4} mol L^{-1} with a detection limit of 9.0×10^{-7} mol L^{-1}.

Keywords: molecularly imprinted polymer, electrochemical sensor, three dimensional ordered macroporous, dopamine, recognition.

1. Introduction

Dopamine (DA), one of the most significant catecholamines in biological organisms with a concentration range of approximately 10^{-7}-10^{-3} mol L^{-1} [1], plays an important role in the functions of the central nervous, cardiovascular, renal and hormonal systems and in drug addiction

and Parkinson's disease [2-3]. However, DA also coexists with high concentrations of other biomolecules in biological samples, which can cause poor selectivities and sensitivities in DA determinations [4-5]. To solve these problems, a variety of electrochemical sensors have been prepared and applied for DA determination in biological samples [6-12]. However, many of these sensors do not meet the growing demand for developing more simple, reliable and efficient sensors with enhanced selectivities and sensitivities for DA detection.

A molecularly imprinted technique [13-15], the design and synthesis of polymers with predetermined recognition capacity to target molecule, has been proposed and developed rapidly in recent years to overcome the limitations of biological recognition system, such as instability against high temperature, organic solvents and pH conditions. The synthesis of molecularly imprinted polymers (MIPs) involves the co-polymerization of functional monomer and cross linker in the presence of template molecule. Extraction of the template molecule from the obtained polymer reveals the complementary binding sites in shape, size, and the position of the functional groups, which can specific rebind and recognize the template molecule from its structure similar compounds [16-19]. Owing to their stability, low cost of preparation, ease of mass production and fitting for wide range of operating conditions, MIPs have been applied in wide fields, such as solid-phase extraction [20-21], chromatographic separation [22-23], catalysis [24-25] and biosensor [11,26]. As promised materials, MIPs also have been used to prepare electrochemical sensor to achieve high selectivity and sensitivity for imprinted molecule simultaneously [27-29].

Although MIPs prepared by conventional methods exhibit high affinity and selectivity to imprinted molecule, some disadvantages were suffered, including the heterogeneous distribution of the binding sites, embedment of mostly binding sites, and poor site accessibility for imprinted molecule. All of these may lead to the low sensitivity and selectivity of sensor if such traditional MIPs were employed as sensing elements. Therefore, facilitating the mass transfer processing and improving the site accessibility are the important issues for MIPs being served as sensor devices.

Based on this consideration, much more researchers have focused on the preparation of nanostructured MIPs, such as thin film, nanospheres, nanowires, and nanotubes [30-34]. In recent years, several techniques have been developed to fabricate the multiporous polymers, including sol-gel techniques, etching techniques, and template techniques. Among these methods, three dimensional ordered macroporous (3DOM) inverse opal structures polymers prepared by the template method have recently received great attention because of their simple process, cost effectiveness, controllable sizes of pore and film thickness [35-39]. Monodispersed spherical colloidal particles are arranged orderly onto the surface substrate in this method. Then the void spaces between particles are filled with fluid precursors, which convert to a solid under certain conditions subsequently. After removal of colloidal particles, the open, interconnected and periodic 3DOM structures can be obtained, providing a high stability, an increase of up to 2 orders of magnitude active surface area compared to that on a flat substrate. If this kind of high periodic macroporous solid was made of MIPs, most of the imprinted sites would situate at the polymers surface or in the proximity of the polymers surface, which should further facilitate the mass transfer of template molecules toward MIPs and increase the utilization of imprinted sites. And this kind of MIPs also can be constructed onto the electrode surface to form a new kind of MIPs electrochemical sensor.

In this article, molecular imprinting and colloidal crystal techniques were combined to fabricate a new kind of electrochemical sensor element onto the glassy carbon electrode (GCE) surface. Monodispersed silica microspheres were naturally settled onto the GCE surface to form a high ordered hard template before it was immersed into prepolymerization solution. Then the polymers were prepared by electropolymerization of pyrrole in the present of DA, one of the most significant catecholamines, which was used as imprinted molecule. After removal of silica colloidal crystal and DA

molecule, the obtained 3DOM MIPs electrochemical sensor exhibited the accessibility of imprinted molecule to the surface imprinted site, and the increase of the mass transport of imprinted molecule. Under the optimized condition, the sensor showed good special adsorption and high recognition capacities to template molecule.

2. Expermental part

2.1. Chemicals

Silica microspheres with diameter of 500 nm were obtained from Alfa Aesar. Dopamine (DA, ≥98.5%), Ascorbic acid (AA, >98%), uric acid (UA, >99%), epinephrine hydrochloride (EP, >98%), and pyrrole were purchased from Fluka (Fluka Chemie AG, Switzerland). Sodium dihydrogen phosphate, sodium phosphate dibasic, and all other reagents were of at least analytical-reagent grade. Double-distilled water was used for all solutions.

2.2. Apparatus

Electrochemical experiments such as cyclic voltammetry (CV), electrochemical impedance spectroscopy (EIS), and differential pulse voltammetry (DPV) were performed on CHI 660C workstation (ChenHua Instruments Co., Shanghai, China) with a conventional three-electrode system. A bare or modified glassy carbon electrode (GCE) was served as a working electrode. A saturated calomel electrode and a platinum wire electrode were used as a reference electrode and a counter electrode, respectively. Field emission scanning electron microscope (FE-SEM) images were obtained on an S-4800 field emission scanning electron microanalyser (Hitachi, Japan).

2.3. Fabrication of silica colloidal crystal template modified GCE (SCCT/GCE)

The preparation of SCCT/GCE was performed by the colloidal crystal template technique. The highly uniform silica colloidal microspheres were dispersed in ethanol under sonication to get a distributed suspension. The side of a clean GCE, wrapped with a tape, was used as a substrate for the colloidal crystal template preparation. The edge of the tape was higher than that of GCE to form a groove. Then a certain amount of silica suspension was introduced into the groove. After the static gravitational sedimentation of silica suspension and evaporation of ethanol, the silica microspheres settled and assembled at the GCE surface, obtaining silica colloidal crystal template modified GCE (SCCT/GCE).

2.4. Preparation of three dimensional ordered macroporous MIPs modified GCE (3DOM-MIPs/GCE)

The SCCT/GCE was immersed into the prepolymerization solution, which was composed of 0.026 mol L^{-1} pyrrole and 0.02 mol L^{-1} DA. After the interspaces of silica crystal template were infiltrated with prepolymerization solution, the cyclic voltametry (CV) was performed from -0.80 V to +1.00 V for several cycles at a scan rate of 100 mV/s, obtaining a polymer modified GCE (SCCT-polymers/GCE). Then the above electrode was incubated into hydrofluoric acid (HF) solution to etch off silica microspheres completely. After washing with water for several times, the electrode was immersed in 0.1mol L^{-1} KCl + 0.05 mol L^{-1} phosphate buffer solution (PBS, pH 7.0) to extract embedded DA by scanning between -0.6 and +1.00 V for several cycles until no obvious oxidation peak of DA could be observed, getting three dimensional ordered macroporous MIPs modified GCE (3DOM-MIPs/GCE). The procedure of fabrication of 3DOM-MIPs/GCE was depicted in Scheme 1.

For comparison, three dimensional ordered macroporous non-molecularly imprinted polymers (NIPs) modified GCE (3DOM-NIPs/GCE) was prepared and treated in exactly the same way, only without addition of DA molecule in the electropolymerization process. And the molecularly imprinted polymers modified GCE (MIPs/GCE) or non-molecularly imprinted polymer modified GCE (NIPs/GCE) were also prepared without SCCT in the construction process, which were used as compared electrodes.

2.5. Electrochemical properties measurements

Electrochemical measurements to characterize the prepared modified electrodes were carried out in 0.05 mol L^{-1} PBS (pH 7.0) by using different

electrochemical techniques including CV, DPV, and EIS. AA, UA, and EP were chosen as the structural similar molecules to evaluate the recognition capacity of the prepared sensor.

3. Results and Discussion

3.1. SEM characterization of 3DOM-MIPs/GCE

The microstructure of 3DOM is highly dependent on the structure of the silica crystal template. In order to fabricate macroporous materials with uniform structure, a key requirement is to prepare well-packed silica microspheres. Sedimentation of silica microspheres using the present method leads to the formation of colloidal crystal template on the surface of GCE. Fig. 1 displayed SEM images of colloidal crystal template formed with silica spheres by sedimentation method (a) and the fabricated MIPs film with an interconnected macroporous structure (b). The monodispersed silica microspheres are regularly stacked on the surface of GCE. This ordered structure is consistent with the colorful appearance of the template. After electropolymerization of MIPs and removal of silica template, 3DOM-MIPs/GCE was obtained as shown in Fig. 1b. The Macropores were interconnected by window channels that are replicated from the partial coalescence necks between the silica spheres. The small dark areas within each pore were the interconnected necks and corresponded to the points of contact of the starting silica microspheres. And the macroporous structure with several layers could be observed in the cross-section high magnification image, as illustrated in the inset of Fig. 1 b.

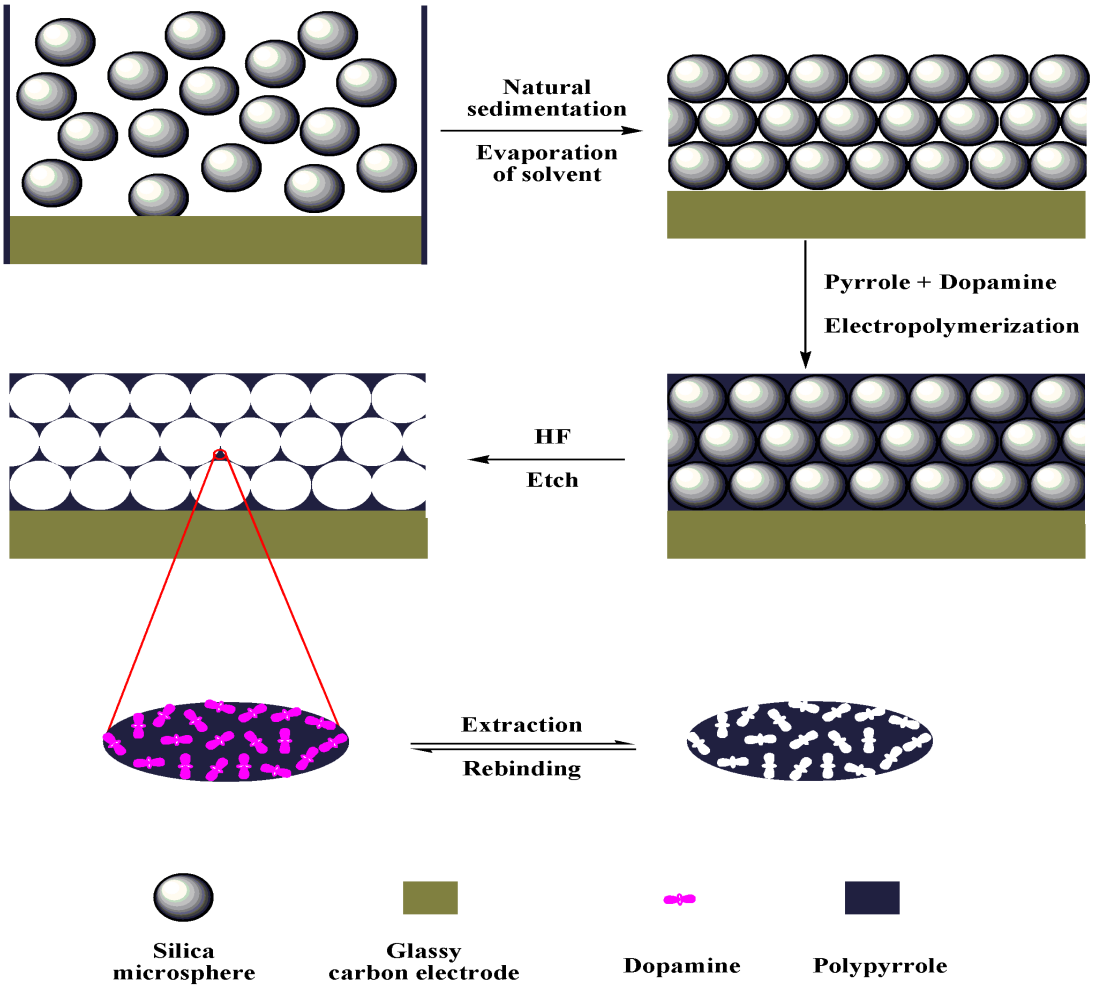

Scheme 1. Scheme of the fabrication of 3DOM-MIPs/GCE

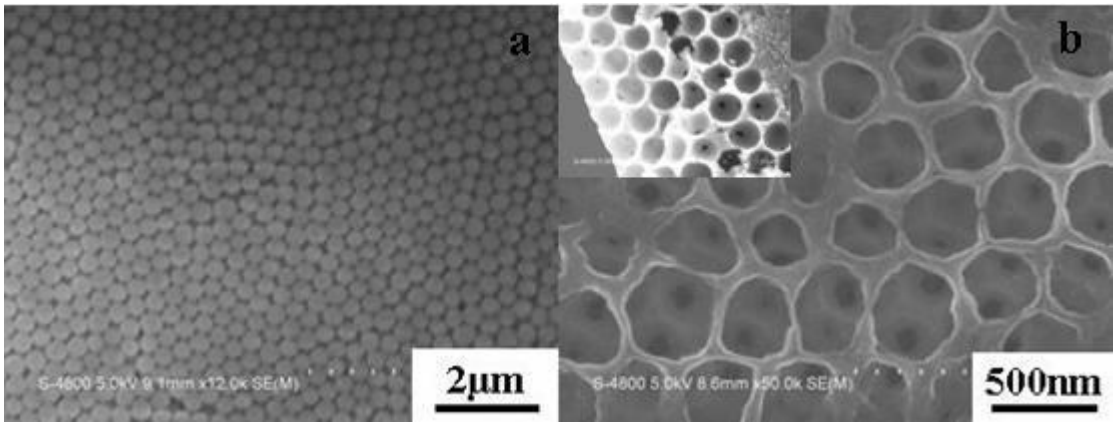

Figure 1. SEM images of SCCT by sediment method (a) and 3DOM-MIPs (b). Inset: cross-section SEM image of 3DOM-MIPs.

3.2. Electrochemical behaviors of 3DOM-MIPs/GCE

3.2.1. EIS characterization of 3DOM-MIPs/GCE

The electrochemical impedance spectroscopy (EIS) was performed to monitor the impedance changes of electrode surface in the modified process. In EIS, a semicircle portion at higher frequencies corresponds to the electron-transfer limited resistance and a linear part at lower frequencies may attribute to the diffusion process. Fig. 2 recorded the Nyquist diagrams of electrode fabricated at each step in the presence of $[Fe(CN)_6]^{3-}/[Fe(CN)_6]^{4-}$. Curve a in Fig. 2 showed the EIS of the bare GCE with a almost straight line, indicating the faster electron-transfer kinetics of $[Fe(CN)_6]^{3-}/[Fe(CN)_6]^{4-}$ on GCE. However, with the coating of silica colloidal crystal template and the subsequent MIPs layer onto the GCE surface (Fig. 2, b and c), the impedances were significantly increased and the semicircle diameters of SCCT/GCE and SCCT-polymers/GCE were about 5.7 and 17.9 KΩ, respectively. This result indicated that SCCT and polymers had the larger obstruction effect, which led to the decrease of electron transfer rate or increase of the resistance of the electron flow.

With the etching off silica template, the semicircle dimater decreased to 3.07 KΩ (Fig. 2 d), which was further reduced to 1.80 KΩ after the extraction of DA (Fig. 2 e). The reason could be that there were large numbers of macropores left by the etch of silica microspheres and imprinted cavities left by the extraction of DA in MIPs layer, which enhanced the diffusion rate of $[Fe(CN)_6]^{3-}/[Fe(CN)_6]^{4-}$ through the MIPs layer and made it easier for the electron-transfer between the electrolyte and the electrode to take place. The impedance changes of the modified process indicated that MIPs film had been modified to the GCE surface successfully. The resistance substantially increased from 1.80 KΩ to 3.70 KΩ (Fig. 2 f), which could be attributed to the rebound DA in imprinted cavities blocking the arrival of $[Fe(CN)_6]^{3-}/[Fe(CN)_6]^{4-}$ to electrode surface.

3.2.2. Specific adsorption of DA toward 3DOM-MIPs/GCE

The electrochemical responses of DA toward different modified electrode were studied using DPV to evaluate the specific adsorption of the sensor, as shown in Fig. 3. An obvious anodic peak was observed at each electrode due to the oxidation of DA. It's apparent that the MIPs modified electrodes displayed much higher current than those of NIPs modified electrode whether SCCT was employed in the sensor prepared process or not, indicating the existence of imprinting cavities in MIPs film. Compared with the MIPs/GCE (Fig. 3c), the peak current of DA on 3DOM-MIPs/GCE (Fig. 3d) increased remarkably, which could be ascribed to the special structured 3DOM-MIPs. Herein, the reproducibility of 3DOM-MIPs/GCE was

investigated for three times with a relative standard deviation of 2.4%.

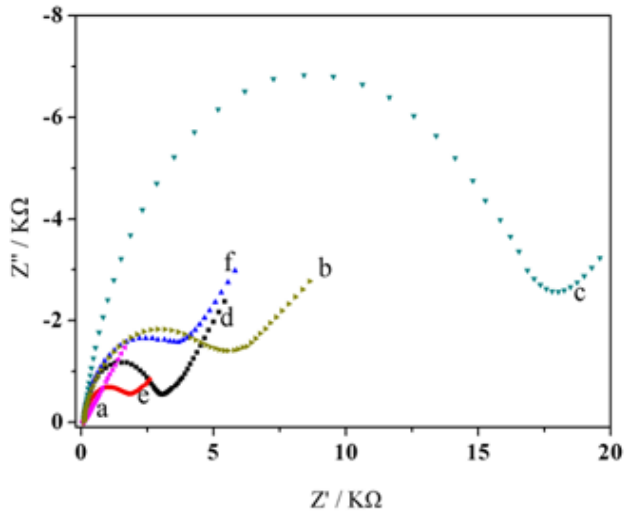

Figure 2. EIS of different modified electrodes recorded in 0.01 mol·L^{-1} $[Fe(CN)_6]^{3-}$/$[Fe(CN)_6]^{4-}$. Bare GCE (a), SCCT/GCE (b), SCCT-polymers/GCE (c), 3DOM-MIPs/GCE before (d) and after (e) extraction of DA, and rebinding 7.7 ×10^{-4} mol L^{-1}DA (f).

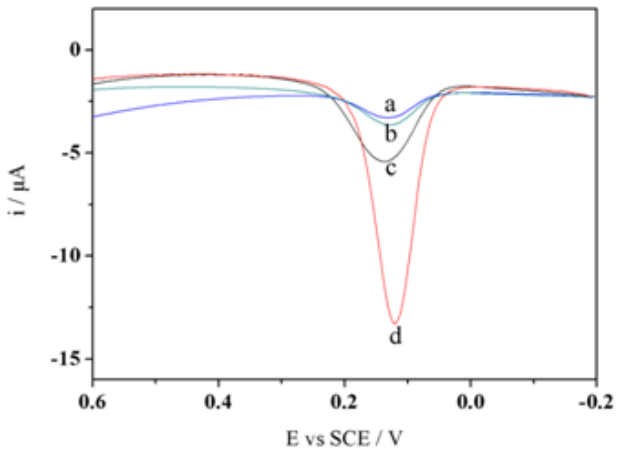

Figure 3. DPV of 2.0×10^{-4} mol L^{-1} DA in PBS at NIPs modified GCE fabricated without (a) and with (b) SCCT, and MIPs modified GCE fabricated without (c) and with (d) SCCT.

The large surface area and thin wall thickness of this structured MIPs enable most imprinting sites to situate at the surface or in the proximity of the surface. The result of adsorption dynamics experiment indicated that the prepared sensor possessed very fast response time within almost 1 min (as shown in Fig. 4), which could be attributed to the better site accessibility and lower mass-transfer resistance of 3DOM-MIPs. Therefore, silica colloidal crystal template method was adopted in the present study could provide much more efficient imprinting cavities and facilitate the adsorption of DA toward MIPs.

And the adsorption isotherm curve was also a common method to study the specific adsorption properties of MIPs. Fig. 5 showed an adsorption isotherm of 3DOM-MIPs/GCE and 3DOM-NIPs/GCE. The binding of DA to 3DOM-MIPs/GCE was compared with 3DOM - NIPs/GCE of DA concentration from 2.0×10^{-6} to 7.7 ×10^{-4} mol L^{-1}. The larger current of each concentration of DA on 3DOM-MIPs/GCE surface than that on 3DOM-NIPs/GCE surface indicated that the 3DOM-MIPs/GCE had specifically binding capacity for imprinted molecule because the imprinted cavities in 3DOM-MIPs are complementary to the size, shape, and functionality of the imprinted molecule.

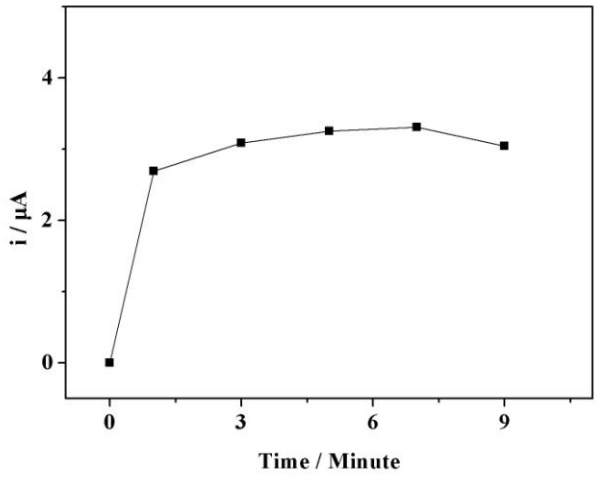

Figure 4. Curve of adsorption dynamics of DA on 3DOM-MIPs/GCE.

3.2.3. Determination of DA

The dependence of the oxidation peak current of DA at 3DOM-MIPs/GCE was investigated by using DPV method. As shown in Fig. 6, it was observed that the current of 3DOM-MIPs/GCE increased with the increase of DA concentration. The calibration graph (the inset of Fig. 6) obtained

for DA determination showed a linear relationship over DA concentration in the range of 2.0×10^{-6} ~ 2.3×10^{-4} mol L^{-1} with correlation coefficient of 0.995. And a limit of detection was measured to be 9.0×10^{-7} mol L^{-1}.

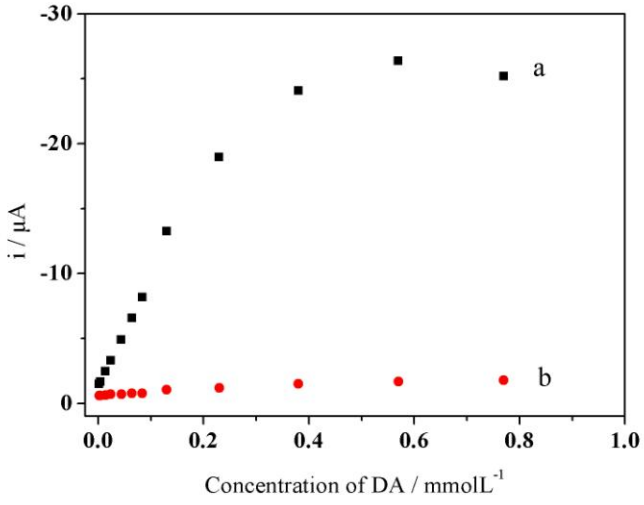

Figure 5. Adsorption isotherms of DA on 3DOM-MIPs/GCE (a) and 3DOM-NIPs/GCE (b).

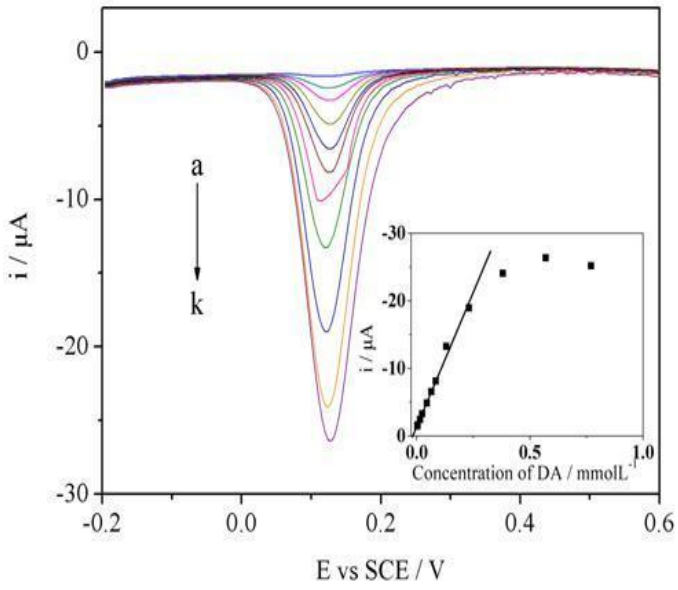

Figure 6. DPV curves on 3DOM-MIPs/GCE with the increase of DA concentration in PBS. Concentration of DA (a): 2.0×10^{-6}, (b): 4.0×10^{-6}, (c): 1.4×10^{-5}, (d): 2.4×10^{-5}, (e): 4.4×10^{-5}, (f): 6.4×10^{-5}, (g):8.4×10^{-5}, (h): 2.3×10^{-4}, (i): 3.8×10^{-4}, (j): 5.7×10^{-4}, (k): 7.7×10^{-4} mol L^{-1}.

3.2.4. Recognition of DA

The selectivity of the proposed sensor was investigated using AA, UA, and EP as the structural analogues. The concentration of the tested compounds was 7.0×10^{-4} mol L^{-1}. Compared with 3DOM-NIPs/GCE, the current value caused by DA on 3DOM-MIPs/GCE was the highest due to the presence of imprinted cavities. The peak currents of other compounds had no substantial change on 3DOM-MIPs/GCE or 3DOM-NIPs/GCE, as shown in Fig. 7. The selectivity of the imprinted sensor to DA was evaluated by calculating the peak current ratio of DA on 3DOM-MIPs/GCE to other analogues under the same conditions. The calculated imprinted ratio of the oxidation current of DA to that of AA, UA, and EP was 12.1, 16.8, and 11.2, respectively. These results confirmed that 3DOM-MIPs/GCE had an excellent selective recognition capacity toward imprinted molecule due to the imprinting effect produced in 3DOM-MIPs, which was electropolymerized in the presence of DA.

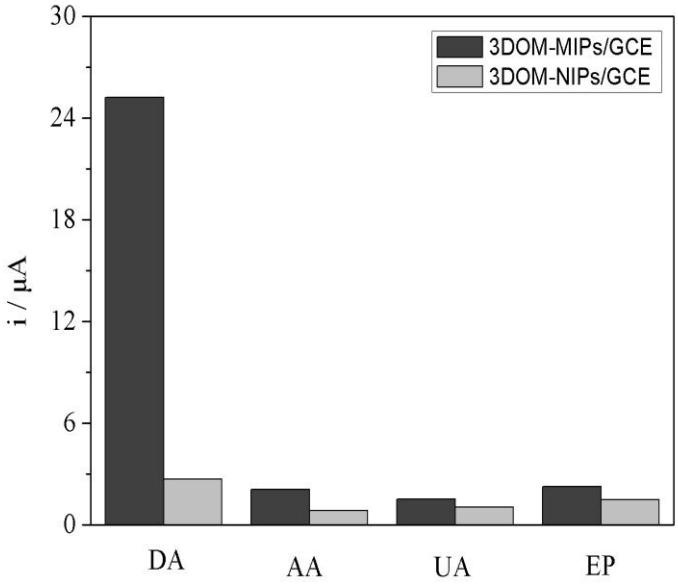

Figure 7. Selectivity of 3DOM-MIPs/GCE.

4. Conclusion

The present study described the development of a novel electrochemical sensor by combining

the molecularly imprinting and colloidal crystal template techniques. Silica microspheres were deposited onto the surface of GCE to form SCCT. Then pyrrole was electropolymerized onto the SCCT/GCE surface in the presence of DA. With the etching of silica microspheres and extracting of DA, the obtained 3DOM-MIPs/GCE possessed multiporous structure and high surface area, which was characterized by SEM. Electrochemical experiments results indicated that the prepared sensor had much more efficient imprinted sites and exhibited a fast binding dynamics, good specific adsorption capacities, and high selective recognition to imprinted molecule. And the sensor was used to detect the concentration of DA with a linear range of 2.0×10^{-6} ~ 2.3×10^{-4} mol L^{-1}. A detection limit was measured to be 9.0×10^{-7} mol L^{-1}.

Acknowledgements

We greatly appreciate the support of the National Natural Science Foundation of China for young program (21005002), Anhui Provincial Natural Science Foundation for Young Program (11040606Q35), Anhui University Provincial Natural Science Foundation Key program (KJ2010A138), Dr Start-up Fundation of Anhui Normal University (160-750834). Dr Start-up Fundation of Anhui Normal University (160-750834).

References

[1] Li, J.; Zhao, J.; Wei, X. A sensitive and selective sensor for dopamine determination based on a molecularly imprinted electropolymer of o-aminophenol, *Sensors and Actuators B: Chemical*, 2009, 140(2), 663-669. DOI:10.1016/j.snb.2009.04.067

[2] Malem, F.; Mandler, D. Self-assembled monolayers in electroanalytical chemistry: application of .omega.-mercapto carboxylic acid monolayers for the electrochemical detection of dopamine in the presence of a high concentration of ascorbic acid, *Analytical Chemistry*, 1993, 65(1), 37-41. DOI:10.1021/ac00049a009

[3] Li, L.Y.; Sun, P.H.; Zhen, X.C. PSD-95 Interacts with Dopamine D1-Receptor: Functional Implication, *American Journal of Biomedical Sciences*, 2011, 3(4), 313-321. DOI:10.5099/aj110400313

[4] Prasad, K. S.; Muthuraman, G.; Zen, J.-M. The role of oxygen functionalities and edge plane sites on screen-printed carbon electrodes for simultaneous determination of dopamine, uric acid and ascorbic acid, *Electrochemistry Communications*, 2008, 10(4), 559-563. DOI:10.1016/j.elecom.2008.01.033

[5] Shang, F.; Zhou, L.; Mahmoud, K. A.; Hrapovic, S.; Liu, Y.; Moynihan, H. A.; Glennon, J. D.; Luong, J. H. T. Selective Nanomolar Detection of Dopamine Using a Boron-Doped Diamond Electrode Modified with an Electropolymerized Sulfobutylether- β -cyclodextrin-Doped Poly(N-acetyltyramine) and Polypyrrole Composite Film, *Analytical Chemistry*, 2009, 81(10), 4089-4098. DOI:10.1021/ac900368m

[6] Schöning, M.J.; Jacobs, M.; Muck, A.; Knobbe, D.T.; Wang, J.; Chatrathic, M.; Spillmann, S. Amperometric PDMS/glass capillary electrophoresis-based biosensor microchip for catechol and dopamine detection, *Sensors and Actuators B: Chemical*, 2005, 108 (1-2), 688-694. DOI:10.1016/j.snb.2004.11.032

[7] Liu, X.; Cheng, L.; Lei, J.; Ju, H. Analyst, Dopamine detection based on its quenching effect on the anodic electrochemiluminescence of CdSe quantum dots, *Analyst*, 2008, 133, 1161-1163. DOI:10.1039/B807183G

[8] Chen, P-Y.; Vittal, R.; Nien, P-C.; Ho, K-C. Enhancing dopamine detection using a glassy carbon electrode modified with MWCNTs, quercetin, and Nafion®, *Biosensors and Bioelectronics*, 2009, 24 (12), 3504-3509. DOI:10.1016/j.bios.2009.05.003

[9] Ciszewski, A.; Milczarek, G. Polyeugenol-modified platinum electrode for selective detection of dopamine in the presence of ascorbic acid, *Analytical Chemistry*, 1999, 71(5), 1055-1061. DOI:10.1021/ac9808223

[10] Zhao, Y.; Gao, Y.; Zhan, D.; Liu, H.; Zhao, Q.; Kou, Y.; Shao, Y.; Li, M.; Zhuang, Q.; Zhu, Z. Selective detection of dopamine in the presence of ascorbic acid and uric acid by a carbon nanotubes-ionic liquid gel modified electrode, *Talanta*, 2005, 66 (1), 51-57. DOI:10.1016/j.talanta.2004.09.019

[11] Lakshmi, D.; Bossi, A.; Whitcombe, M. J.; Chianella, I.; Fowler, S. A.; Subrahmanyam, S.; Piletska, E. V.; Piletsky, S. A. Electrochemical Sensor for Catechol and Dopamine Based on a Catalytic Molecularly Imprinted Polymer-Conducting Polymer Hybrid Recognition Element, *Analytical Chemistry*, 2009, 81 (9), 3576-3584. DOI:10.1021/ac802536p

[12] Wang, Y.; Zhang, X.H.; Chen, Y.; Xu, H.; Tan, Y.M.; Wang, S.F. Detection of Dopamine Based on Tyrosinase-Fe_3O_4 Nanoparticles-chitosan Nanocomposite Biosensor, *American Journal of Biomedical Sciences, 2010, 2(3), 209-216.* DOI:10.5099/aj100300209

[13] Wulff, G. Molecular Imprinting in Cross-Linked Materials with the Aid of Molecular Templates— A Way towards Artificial Antibodies, *Angewandte. Chemie International Edition*, 1995, 34 (17), 1812-1832. DOI:10.1002/anie.199518121

[14] Vlatakis, G.; Andersson, L.; Mosbach, I.K. Drug assay using antibody mimics made by molecular imprinting, *Nature*, 1993, 361, 645-647. DOI:10.1038/361645a0

[15] Sellergren, B. Molecularly imprinted polymers: Shaping enzyme inhibitors, *Nature Chemistry*, 2010, 2 (1) 7-8. DOI:10.1038/nchem.496

[16] Hoshino, Y.; Koide, H.; Urakami, T.; Kanazawa, H.; Kodama, T.; Oku, N.; Shea, K. J. Recognition, Neutralization, and Clearance of Target Peptides in the Bloodstream of Living Mice by Molecularly Imprinted Polymer Nanoparticles: A Plastic Antibody, *Journal of American Chemistry Society*, 2010,132 (19), 6644-6645. DOI:10.1021/ja102148f

[17] Liang, Y.; Gu, L.; Liu, X.; Yang, Q.; Kajiurs H.; Li, Y.; Zhou, T.; Shi, G. Composites of Polyaniline Nanofibers and Molecularly Imprinted Polymers for Recognition of Nitroaromatic Compounds, *Chemistry-A European Journal*, 2011, 17(21), 5989-5997. DOI:10.1002/chem.201002709

[18] Chen, Z.; Xu, L.; Liang, Y.; Zhao, M. pH-Sensitive Water-Soluble Nanospheric Imprinted Hydrogels Prepared as Horseradish Peroxidase Mimetic Enzymes, *Advanced Materials*, 2010, 22 (13), 1488-1492. DOI:10.1002/adma.200903122

[19] Kan, X.; Zhao, Q.; Shao, D.; Geng, Z.; Wang, Z.; Zhu, J-J. Preparation and Recognition Properties of Bovine Hemoglobin Magnetic Molecularly Imprinted Polymers, *The Journal of Physical Chemistry. B*, 2010, 114 (11), 3999-4004. DOI:10.1021/jp910060c

[20] Zhou, J.; Ma, C.; Zhou, S.; Ma, P.; Chen, F.; Qi, Y.; Chen, H. Preparation, evaluation and application of molecularly imprinted solid-phase microextraction monolith for selective extraction of pirimicarb in tomato and pear, *Journal of Chromatography A*, 2010, 1217 (48), 7478-7483. DOI:10.1016/j.chroma.2010.09.079

[21] Wang, B.; Wang, Y.; Yang, H.; Wang, J.; Deng, A. Preparation and characterization of molecularly imprinted microspheres for selective extraction of trace melamine from milk samples, *Microchimica Acta*, 2011, 174 (1-2), 191-199. DOI:10.1007/s00604-011-0613-4

[22] S. Ambrosini, M. Serra, S. Shinde, B. Sellergren, E. De Lorenzi. Synthesis and chromatographic evaluation of molecularly imprinted polymers prepared by the substructure approach for the class-selective recognition of Glucuronides, *Journal of Chromatography A*, 2011,1218 (39), 6961-6969. DOI:10.1016/j.chroma.2011.07.104

[23] Rodríguez, E.; Navarro-Villoslada, F.; Benito-Peña, E.; Marazuela, M. D.; Moreno-Bond, M. C. Multiresidue Determination of Ultratrace Levels of Fluoroquinolone Antimicrobials in Drinking and Aquaculture Water Samples by Automated Online Molecularly Imprinted Solid Phase Extraction and Liquid Chromatography, *Analytical Chemistry*, 2011, 83(6), 2046-2055. DOI:10.1021/ac102839n

[24] Strikovsky, A. G.; Kasper, D.; Grün, M.; Green, B. S.; Hradil, J.; Wulff, G. Catalytic Molecularly Imprinted Polymers Using Conventional Bulk Polymerization or Suspension Polymerization: Selective Hydrolysis of Diphenyl Carbonate and Diphenyl Carbamate, *Journal of American Chemistry Society*, 2000, 122 (26), 6295-6296. DOI:10.1021/ja994269y

[25] Abbate, V.; Bassindale, A. R.; Brandstadt, K. F.; Taylor, P. G. Biomimetic catalysis at silicon centre using molecularly imprinted polymers, *Journal of Catalysis*, 2011, 284 (1), 68-76. DOI:10.1016/j.jcat.2011.08.019

[26] Jing, T.; Xia, H.; Niu, J.; Zhou, Y.; Dai, Q.; Hao, Q.; Zhou, Y.; Mei, S. Determination of

trace 2,4-dinitrophenol in surface water samples based on hydrophilic molecularly imprinted polymers/nickel fiber electrode, *Biosensors and Bioelectronics*, 2011, 26 (11), 4450-4456. DOI:10.1016/j.bios.2011.05.001

[27] Yang, Q.; Sun, Q.; Zhou, T.; Shi, G.; Jin, L. Determination of Parathion in Vegetables by Electrochemical Sensor Based on Molecularly Imprinted Polyethyleneimine/Silica Gel Films, *Journal of Agriculture Food Chemistry*, 2009, 57 (15), 6558-6563. DOI:10.1021/jf901286e

[28] Pietrzyk, A.; Suriyanarayanan, S.; Kutner, W.; Chitta, R.; Souza, F. D. Selective Histamine Piezoelectric Chemosensor Using a Recognition Film of the Molecularly Imprinted Polymer of Bis(bithiophene) Derivatives, *Analytical Chemistry*, 2009, 81 (7), 2633-2643. DOI:10.1021/ac8025652

[29] Mao, Y.; Bao, Y.; Gan, S.; Li, F.; Niu, L. Electrochemical sensor for dopamine based on a novel graphene-molecular imprinted polymers composite recognition element, *Biosensors and Bioelectronics*, 2011, 28 (1), 291-297. DOI:10.1016/j.bios.2011.07.034

[30] Lu, Y.; Yan, C-L.; Wang, X-J.; Wang, G-K. Protein imprinting and recognition via forming nanofilms on microbeads surfaces in aqueous media, *Applied Surface Science*, 2009, 256 (5) 1341-1346. DOI:10.1016/j.apsusc.2009.08.003.

[31] Gao, R.; Kong, X.; Wang, X.; He, X.; Chen, L.; Zhang, Y. Preparation and characterization of uniformly sized molecularly imprinted polymers functionalized with core–shell magnetic nanoparticles for the recognition and enrichment of protein, *Journal of Materials Chemistry*, 2011, 21, 17863-17871. DOI:10.1039/C1JM12414E

[32] Yang, H-H.; Zhang, S-Q.; Tan, F.; Zhuang, Z-X.; Wang, X-R. Surface Molecularly Imprinted Nanowires for Biorecognition, *Journal of American Chemistry Society*, 2005, 127 (5), 1378-1379. DOI:10.1021/ja0467622

[33] Xie, C.; Zhang, Z.; Wang, D.; Guan, G.; Gao, D.; Liu, J. Surface Molecular Self-Assembly Strategy for TNT Imprinting of Polymer Nanowire/Nanotube Arrays, *Analytical Chemistry*, 2006, 78 (24), 8339-8346. DOI:10.1021/ac0615044

[34] Chronakis, I. S.; Milosevic, B.; Frenot, A.; Ye, L. Generation of Molecular Recognition Sites in Electrospun Polymer Nanofibers via Molecular Imprinting, *Macromolecules*, 2006, 39 (1), 357-361. DOI:10.1021/ma052091w

[35] Holland, B. T.; Blanford, C. F.; Stein, A. Synthesis of Macroporous Minerals with Highly Ordered Three-Dimensional Arrays of Spheroidal Voids, *Science*, 1998, 281 (5376), 538-540. DOI:10.1126/science.281.5376.538

[36] Holland, B. T.; Blanford, C. F.; Do, T.; Stein, A. Synthesis of Highly Ordered, Three-Dimensional, Macroporous Structures of Amorphous or Crystalline Inorganic Oxides, Phosphates, and Hybrid Composites, *Chemistry of Materials*, 1999, 11 (3) 795-805. DOI:10.1021/cm980666g

[37] Hu, X.; An, Q.; Li, G.; Tao, S.; Liu, J. Imprinted Photonic Polymers for Chiral Recognition, *Angewandte Chemie International Edition*, 2006, 45 (48), 8145-8148. DOI: 10.1002/anie.200601849

[38] Berhanu, S.; Tariq, F.; Jonesm, T.; McComb, D. W. Three-dimensionally interconnected organic nanocomposite thin films: implications for donor–acceptor photovoltaic applications, *Journal of Material Chemistry*. 2010, 20, 8005-8009. DOI: 10.1039/c0jm01030h

[39] Xue, M. J.; Xiao, W. T.; Zhang, Z. J. Porous Films from Transformation of Polymeric Sphere Arrays, *Advanced Materials*. 2008, 20 (3) 439-442. DOI: 10.1002/adma.200702015

